ARPA-E Quarterly Technical Report
Award - DE-AR0001559
Quarter 4 (May 1, 2023 – July 31, 2023)

Project Title: Quantifying the Potential and Risks of Large-Scale Macrophyte Cultivation and Purposeful Sequestration as a Viable CO2 Reduction (CDR) Strategy (SeaweedCDR)

This is the fourth quarterly report for the SeaweedCDR project, covering the period May 1 to July 31, 2023. As you should recall, we had an issue in completing M2.1 (Design & Implement Seaweed Packaging) as planned due to the lack of large quantities of giant kelp biomass available for purchase. This temporality impacted our progress and pushed back this deliverable, as well as the next deliverable M2.2 (Seaweed Biomass Fates Methods Development), a quarter. We have recovered from that and have completed M2.1 this quarter and are on track to completing M2.2 next quarter. The other deliverables for this quarter are M3.2 (Demonstration of precision of DOC methods - a go/no go milestone) and M4.3 (Streamlining the macroalgal growth model). Both of these are milestones have been being completed successfully and on schedule.

Task 2 – Quantification of Seaweed Biomass Fates
Q4 deliverable – M2.1 – Design and Implementation of Seaweed Packaging – Completion level 100%

Leads: Sebastian Krause, Bob Miller & David Valentine (UCSB)

This quarter we were able to finish and fulfill the M2.1 milestone "design and implementation of seaweed packaging". As part of fulfilling task M2.1 this quarter, we have completed and uploaded our white paper to EarthARXiv (Krause et al. 2023). The "packaging" white paper describes four conveyance methods that we developed to get *Macrocystis* biomass to the seafloor and in what setting each method would be implemented through both lab and field experiments. Since the winter season, only small batches of kelp have been available, which we have used to implement small scale packaging designs in laboratory settings (i.e., whole frond and masticated kelp biomass). As previously mentioned in previous quarterly reports, the depleted density of the local kelp forests off the coast of Santa Barbara temporarily impacted our ability to implement field experiments of our larger package designs (i.e., baling). However, recovery of local *Macrocystis* kelp forests have allowed us to implement bailing packaging designs in the field.

We designed and developed two types of kelp packages that we deployed on May 31st, 2023 within the Santa Barbara Basin. The two types of kelp packages differ in material and surface area to volume. The first package type consisted of a plastic milk crate (13” X 13” X 11”, L X W X H), lined with ¾” nylon mesh, weighted with lead (20 lbs), and equipped with sonar reflectors (two HDPE bucket lids and reflective flag) and reflective tape (Fig. 1A and B). The second type of package consisted of two kelp-filled biodegradable burlap bags that are mounted to a natural

jute line mooring. The kelp-filled burlap sacks were weighted with a burlap sack filled with locally-sourced stones that could be released from the mooring via a pin release system (Fig. 1C and D). These packages would then be recovered from the seafloor by *HOV Alvin* during a research expedition within the Santa Barbara Basin on board the *R/V Atlantis* (see next section for additional details).

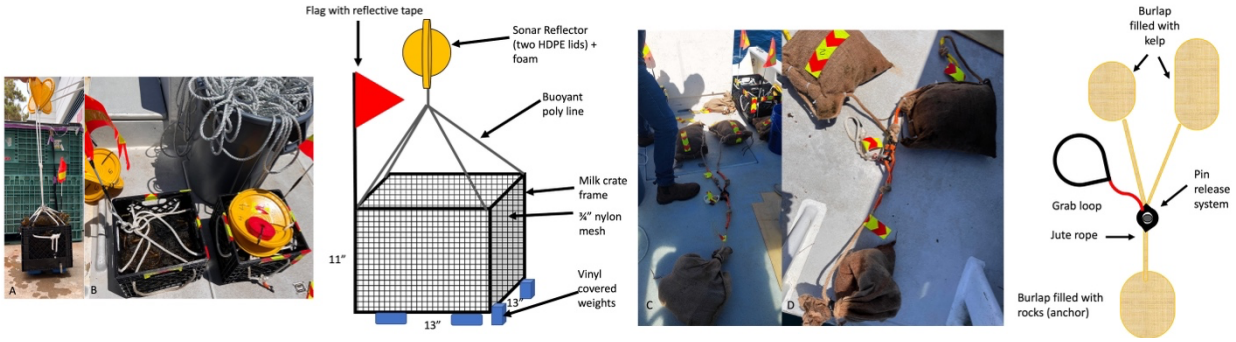

Figure 1. Photos and schematics of milk crate packages (A and B) and burlap sack mooring (C and D) placed at the seafloor of the Santa Barbara Basin.

Prior to package placement on the seafloor, both types of packages were filled with *Macrocystis* kelp. The milk crates contained between 10-15 lbs of kelp. For the jute rope mooring two burlap sacks were filled with kelp; 1) filled half full (~7 lbs of kelp), 2) filled full (~18 lbs of kelp). The kelp packages were then deployed at two locations within the Santa Barbara Basin, Northern Depositional Radial Origin (NDRO) and Northern Depositional Transect 3- station D (NDT3-D) (Fig. 2A). At each station two milk crate packages and one burlap sack-jute rope mooring were deployed by hand off a UCSB boat (Fig. 2B). The two stations were selected for this work because they provided the greatest differences in water column depth (585 meters at NDRO; 447 meters at NDT3-D), oxygen concentrations in the bottom water (NDRO < 5 µM vs NDT3-D ~10 µM), and potential biological interactions (NDRO contained dense microbial mats and hardly any active mega/macro fauna vs NDT3-D contained more active mega/macro fauna and no microbial mats).

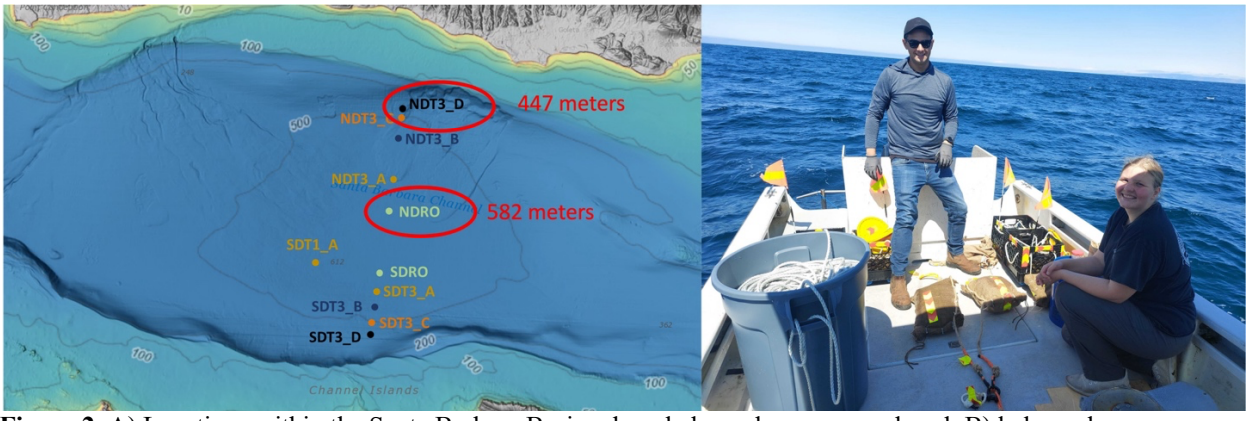

Figure 2. A) Locations within the Santa Barbara Basin where kelp packages were placed; B) kelp package placement off UCSB Fish boat.

Research Expedition to the Santa Barbara Basin (AT50-11)

At the time of writing this report, we just concluded a 3-week research expedition (June 22 till July 12, 2023) within the Santa Barbara Basin on board the *R/V Atlantis* (Fig. 3A). Our goals were three-fold: 1) locate, sample, and recover kelp packages and natural kelp falls within the Santa Barbara Basin using *HOV Alvin* (Fig. 3B); 2) observe and record biological and environmental interactions of the kelp packages and natural kelp falls within the Santa Barbara Basin using *HOV Alvin*; 3) Conduct kelp degradation experiments using sample bag methods that we developed in the laboratory.

Figure 3. A) Research Vessel Atlantis at port; B) ARPA-e team in front of the Human Operated Vehicle Alvin within a hanger on board the Research Vessel Atlantis.

With *HOV Alvin* we were able to locate the kelp packages (two milk crates and burlap sacks) placed at NDRO (Fig. 4A and C). They were found within 20-25 meters from the surface drop coordinates. With high-definition cameras mounted on *HOV Alvin* we recorded video and photographed the kelp packages. Sediment samples were collected around the kelp packages using push cores. The sediment samples from around the milk crate kelp packages were processed by our UCLA collaborators (Treude Laboratory) on board the *R/V Atlantis* for porewater geochemistry, radiotracer incubations and microbial analysis (Fig 4D). We plan to compare the geochemistry results found around the milk crates to geochemistry results where kelp was not present to better understand the environmental impact of placing kelp biomass in anoxic sediments. Unfortunately, sediment samples could not be obtained around the burlap sack jute mooring at NDRO because the sediments around the burlap sacks were heavily disturbed during the search for the packages with *HOV Alvin*. Both the kelp burlap sacks (Fig. 4B), and the milk crate packages (Fig. 4E) were recovered from the seafloor using *HOV Alvin* and then sampled shortly after *HOV Alvin* was recovered on board the *R/V Atlantis*.

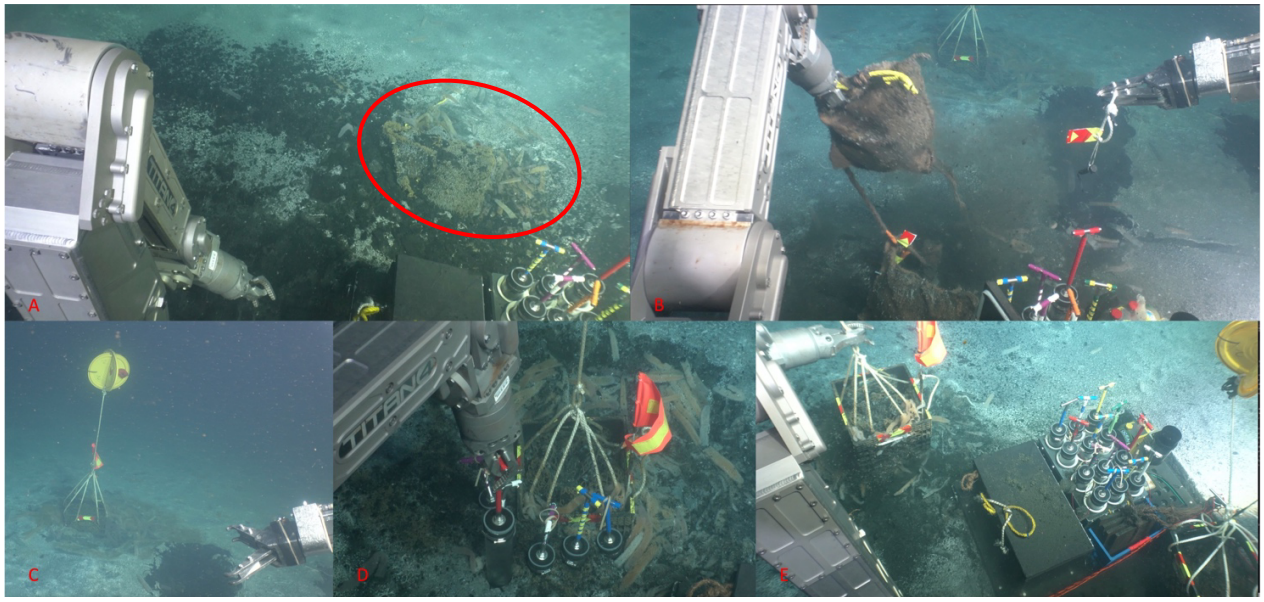

Figure 4. Images of burlap (red circle) (A) and milk crate (C) kelp packages on the seafloor at NDRO. B) *HOV Alvin* releasing kelp filled burlap sack from the rock-filled burlap sack; D) Sediment sampling using pushcores around the milk crate using *HOV Alvin*'s manipulator; E) Milk crate kelp package recovered from the seafloor at NDRO using *HOV Alvin*'s manipulator.

Samples for dissolved organic carbon (DOC) concentrations were collected from the burlap's sacks (Fig. 5A) but not from the milk crates. Unfortunately, during the recovery of *HOV Alvin* back onto the deck of *R/V Atlantis* much of the leftover kelp inside the milk crates got washed out of the crates due to surface waves and currents. This limited our ability to sample and preserve kelp tissue samples from the milk crates. The state of the packages and of the kelp tissue, after sitting on the seafloor for 5 weeks, were photographed and tissue samples from both packages were preserved for microbial analysis (Fig. 5). Kelp packages that were placed at the NDT2-D station (Fig. 2A), were not located by *HOV Alvin*. The seafloor where we believe the packages to have landed was extensively searched by *HOV Alvin*, which was equipped with sonar technology (~100-meter radius from the drop coordinates over three separate dives). It is unclear as to what happened to, or the whereabouts of, the kelp packages as poor visibility limited our ability to look for clues or signs of the kelp packages.

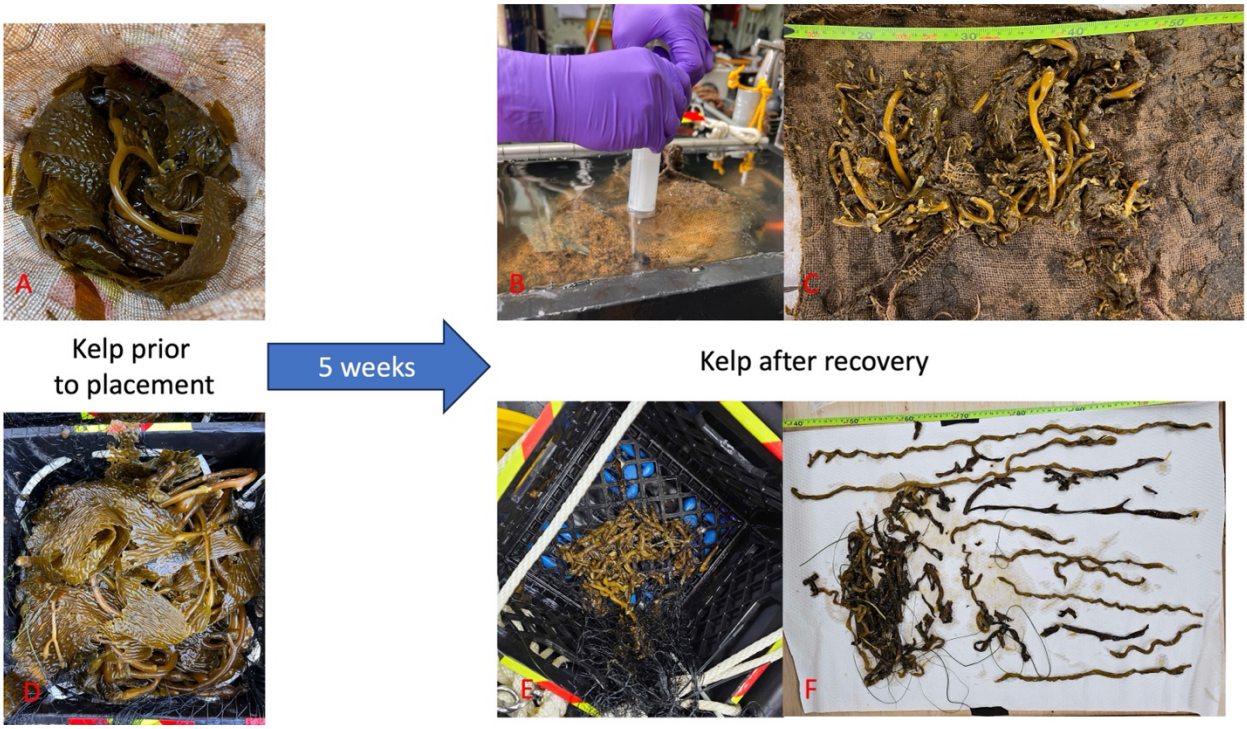

Figure 5. Comparison of the kelp in the packages before deployment (A and D) and after recovery by *HOV Alvin* (B, C, E, and F). Sampling the liquid within the burlap kelp package with a needle and syringe (B). Residual kelp biomass in one of the burlap sacks (C) and in one of the milk crate packages (F) recovered from NDRO.

Natural kelp falls were also observed at the seafloor of the Santa Barbara Basin during *HOV Alvin* dives (Fig. 6). These natural kelp falls were video-recorded prior to sampling from the seafloor (Fig. 6A). Kelp tissue that was brought to the surface was subsampled for microbial analysis and inspected under a dissection microscope to observe and record macrofaunal grazing (Fig. 5C - F). Figure 5F shows a piece of kelp biomass that appears to be damaged by grazing. Species of gastropod (Fig. 5C) and arthropods (Fig. 5D and E) were observed on the kelp holdfast tissue and show that the kelp biomass is a food source for invertebrates on the seafloor. Tissue samples of the kelp and the invertebrates were subsampled for future identification and isotope analysis. These observations are the first steps towards understanding the macrofaunal interactions with kelp biomass and inform how we plan to observe other macrofaunal interactions as part of task M2.6.

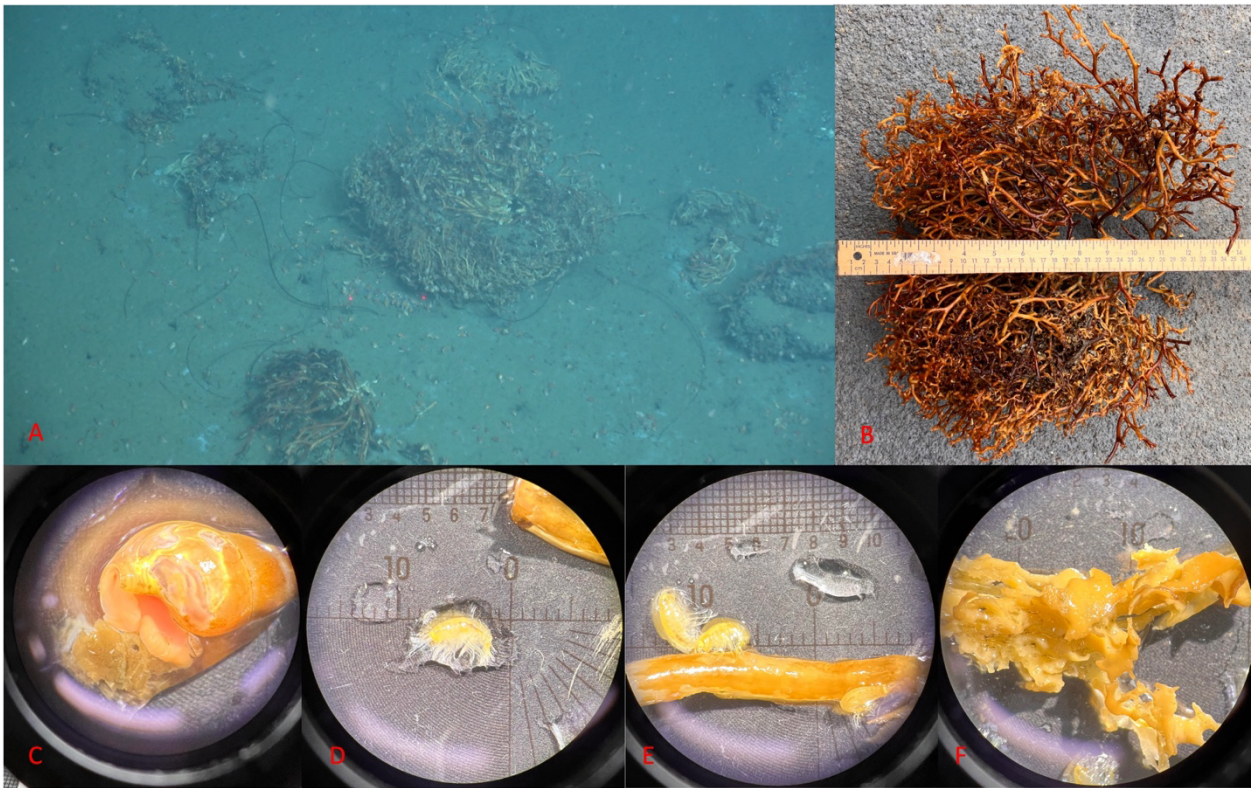

Figure 6. A) *Macrocystis pyrifera* holdfast found on the seafloor of the Santa Barbara Basin; B) *Macrocystis pyrifera* holdfast on deck of the *R/V Atlantis*; C) Unidentified gastropod with kelp tissue; D) Unidentified arthropod; E) Unidentified arthropod on *Macrocystis pyrifera* holdfast tissue; F) Grazing patterns on *Macrocystis pyrifera* holdfast tissue.

We took the opportunity to conduct kelp degradation experiments on board the *R/V Atlantis* to make progress on tasks M2.2, 2.3, 2.5 and 2.6. For this experiment, one week prior to the expedition fresh *Macrocystis* kelp fronds were collected off the coast of Santa Barbara by UCSB scientific divers. The *Macrocystis* kelp fronds were kept alive in a wet lab facility on the UCSB campus (Fig. 7A) and then transported on ice to the *R/V Atlantis*. The *Macrocystis* kelp fronds were then held in a cooler placed on the deck of the *R/V Atlantis* with constant flowing seawater which allowed us to have the freshest kelp possible for our experiments (Fig. 7B). Heat sealable poly-nylon plastic bags were equipped with valves that enables subsampling of the seawater inside the bags over time (Fig. 7 C and D). *Macrocystis* kelp fronds were dissected into components (blades, stipe and pneumatocysts) and placed into the poly-nylon bags. The poly-nylon plastic bags with kelp where then heat-sealed and then flushed three times with ultra-high pure nitrogen (Airgas) to remove residual air from the bags. Anoxic seawater from NDRO was collected with 10L niskin bottles on a rosette equipped with a CTD supplied by the *R/V Atlantis*. Anoxic seawater was directly transferred from the niskin bottles into the heat-sealed sample bags containing kelp biomass through the sample valves without exposing the seawater to the atmosphere. The seawater within the bags were then subsampled and preserved for DOC (Fig. 7E), dissolved inorganic carbon (DIC), and particulate organic carbon (POC) over time.

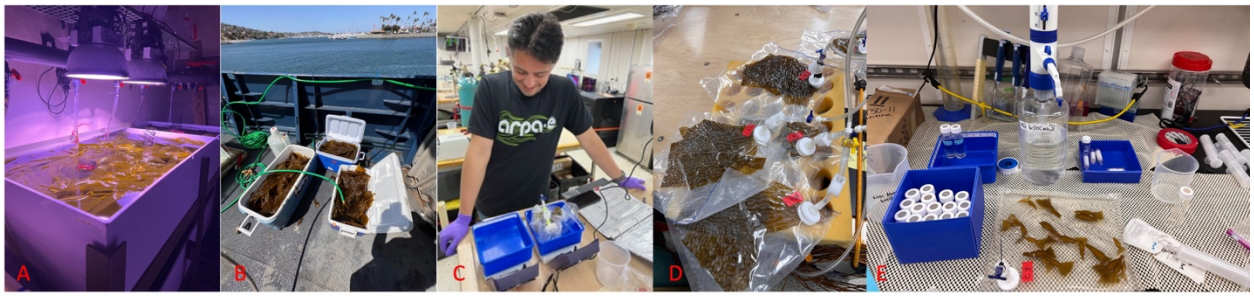

Figure 7. A) Fresh kelp held in holding tank in wet lab on the UCSB campus; B) Live kelp held in coolers flushed with seawater on the deck of the *R/V Atlantis*; C) Sample bag preparation in the on-board lab space; D) Nitrogen flushing of heat sealable poly nylon plastic bags containing *Macrocysistis* biomass; E) Subsampling of seawater from poly nylon plastic bags containing *Macrocysistis* biomass for DOC analysis.

Task 2 current and upcoming plans

This summer we plan to conduct more field work to sink larger quantities (>500 lbs) of kelp using the slinky trap setup described in previous quarterly reports. Additionally, we plan to develop, document, and implement sinking rate experiments in the field and in the laboratory to better understand the sinking rates of kelp fronds and kelp packages as part of task M2.2 and 2.4. This summer we will work closely with the Carlson lab and the Marine Science Institute Analytical Laboratories at UCSB to develop and document protocols to analyze DIC, DOC, and POC samples to fulfill components of tasks M2.2, 2.3, 2.5, and 2.6.

Task 3 – Quantification of Seaweed DOM Fates

Q4 deliverable – M3.2 – Demonstration of precision of outlined protocols to measure DOC release rates, composition and remineralization rates – Completion level 100%

Leads: Chance English & Craig Carlson (UCSB)

For M3.2 we report on the precision of our previously outlined in English and Carlson 2023 (SOPO 3.1; Earth ArXiv; DOI:10.31223/X5167F) to measure and model the release rate of DOC, its composition and remineralization rate. We report on preliminary results showing these protocols meet the criteria defined in M3.2. Release rates from 9 replicate incubations show a significant positive relationship with productivity. The composition of DOC from 8 *Macrocystis* blades show that carbohydrates and polyphenols are 54% of the kelp derived DOC. Carbohydrates are enriched in fucose, galactose, glucuronic acid and sulfate, indicating fucoidan is an important component of giant kelp exudates. The production of polyphenols by giant kelp results in changes to seawater optical properties in the UV range. The increase in absorption is strongly correlated with macroalgal DOC concentrations and could provide a useful tracer for macroalgal DOC in an aquaculture setting. Lastly, we define methods to determine the recalcitrance of seaweed DOC based on its molecular properties, community composition and environmental variables (nutrients, temperature, light). We note that the remineralization experiments used to constrain the recalcitrance of Kelp derived DOC, outlined in our protocols,

require timescales greater than the period of quarterly reporting. As a result, we cannot yet show results from DOC remineralization experiments from *Macrocystis pyrifera*. However, as a proof of concept, we present results on the remineralization of DOC from *Sargassum natans*, another brown macroalgae, carried out between 2021-2022 using the same methods outlined in SOPO 3.1. Results from this remineralization experiment demonstrate a recalcitrant component of macroalgal DOC, possibly due to high concentrations of polyphenols.

Determination of DOC Release Rates

Seaweed Incubation Design - To test our incubation design, mature blades were collected from Mohawk Reef in Santa Barbara, California and transported back to UCSB in surface seawater. Blades were collected 2m back from the meristem of two growing fronds to ensure samples were physiologically similar. Blades were placed in 10L acrylic incubation tanks with 0.2 µm filtered seawater and magnetic stir bars to maintain flow. Incubations were conducted in triplicate at six different light levels for two hours. Blades were allowed 20 minutes to acclimate to the incubation conditions in order to prevent sampling of exudation driven by rapid changes to temperature or salinity (Carlson and Carlson 1984; Zhao et al. 2023).

Preliminary Results - Our incubation design captures a typical relationship between NPP and light intensity. We also find that DOC release rates show a similar relationship to light as NPP (Figure 8a). A hyperbolic-tangent model explained 98% of the variability in photosynthesis and 80% of the variability in DOC production. This suggests, that under constant environmental conditions with blades of a similar age, light is an important factor which could be used to model DOC production within 20% of our measured values. DOC release increased linearly with NPP (Figure 8b), and the proportion of NPP released as DOC was consistent (~3 ± 0.8%) across all light levels when irradiance > 0. DOC release continued in the dark and could represent an important loss of NPP during the night.

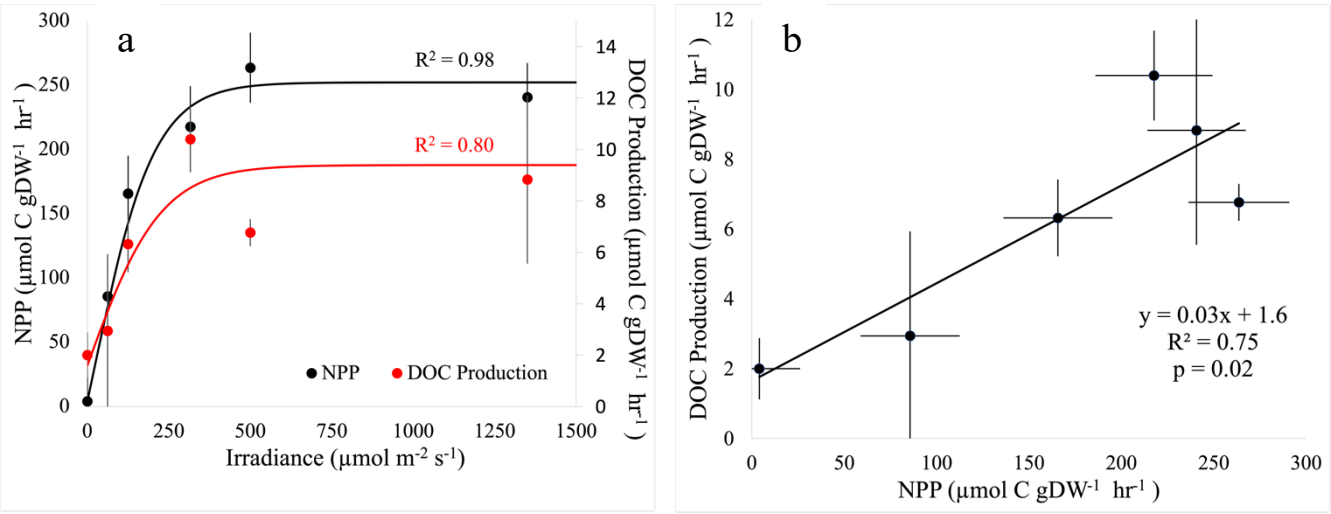

Figure 8. (a) DOC production and NPP light curves. Solid lines are modeled NPP and DOC production using a hyperbolic tangent function. R^2 values from Model I linear regression compare predicted and measured rates (solid circles). (b) DOC release increases with NPP. Inset is results of model II linear regression.

We performed an additional experiment using blades at different lengths from the apical meristem as a proxy for age. Duplicate blades from 0.1, 1 and 2m from the growing tip were incubated under constant saturating light (PAR = 500 µmol m^{-2} s^{-2}) for 3 hours. Under constant saturating light, we observed a significant negative relationship between photosynthesis and distance from the tip (Figure 9a) and DOC release and distance from the tip (Figure 9b). Therefore, blade age may modulate the relationship between light and DOC release. We note that the distance along the frond we used roughly translates to only about 14 days which is small relative to the ~100-day lifespan of giant kelp blades. On-going work is evaluating DOC release along a more representative age range and will evaluate the control of light along this physiological gradient.

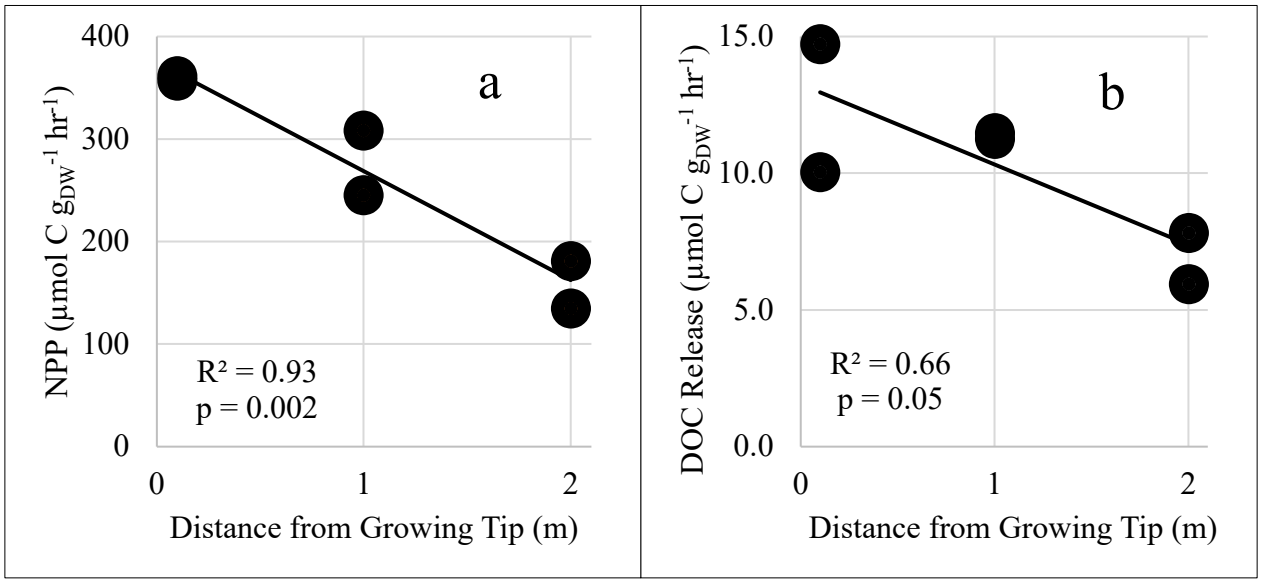

Figure 9. (a) Net primary production and (b) DOC release rates across a blade age gradient under constant light intensity. Distance from tip used as a proxy for age with greater distance meaning older blades. Solid lines and insets are Model I regression results.

Precision - Coefficients of variation of the replicate incubations (n=9) described above averaged 11 and 29% for average NPP and DOC release rates, respectively using our incubation design. The average variation for DOC release rates is above the target 20% outlined in SOPO 3.2, however we note that 5 out of the 9 replicated incubations have a coefficient of variation below 20%. Moreover, our work with mature, clipped giant kelp blades show DOC release rates from 1.7 – 14 µmolC g_{DW} hr^{-1}, comparable to rates observed by Reed et al. 2015 (0-12.5 µmolC g_{DW} hr^{-1}) who used sleeved incubations of giant kelp blades without clipping. This suggests that our laboratory experiments yield DOC release rates similar to observed *in situ* rates.

Determination of Seaweed DOM Composition

Compounds & Methods - We are focusing on two classes of compounds: Carbohydrates and Polyphenols which are large components of seaweed DOC and contain potentially recalcitrant components (Jennings and Steinberg 1994; Abdullah and Fredriksen 2004; Wada et al. 2007; Nelson 2013; Powers et al. 2019). Carbohydrates, total phenol content and DOC optical properties are measured by High-Performance Anion-Exchange Chromatography with Pulsed Amperometric Detection (HPAEC-PAD) (Engel and Händel 2011), the Folin-Ciocâlteu method (Box 1983; Takeda et al. 2013; Powers et al. 2019) and UV-Vis spectroscopy (Shank et al. 2010), respectively.

Sulfate Content - Fucoidan makes up 18-50% of brown macroalgal DOC (Buck-Wiese et al., 2023). These large polysaccharides are highly sulfated and difficult to degrade due to the diversity of enzymes required to remove sulfate groups, hydrolyze glycosidic linkages, and metabolize fucose (Sichert et al., 2020). These fucoidans have a range in sulfate content (Sichert et al., 2021), which may change their bioavailability. The sulfate content of macroalgal exudates can be determined following the procedure to measure sugar monomers by HPAEC-PAD (Section 2.1). Following dialysis, hydrolysis, and neutralization, liberated sulfate from the hydrolysis of sulfate] ester groups can be measured by ion chromatography.

Preliminary Results - Using the set up described above, 8 *Macrocystis* blades were incubated at a single PAR level and the resulting DOC compounds were collected and characterized using HPAEC-PAD and the Folin-Ciocâlteu colorimetric method for carbohydrates and polyphenols, respectively. Carbohydrates and polyphenols comprised 30 ± 21% and 24 ± 16% (54% total) of the accumulated DOC. Specific sugars are dominated by fucose and galactose and glucuronic acid which are thought to be sourced from fucoidan (Buck-Wiese et al. 2023). Sulfate content of a single sample was measured, in quadruplicate and occurred at a molar ratio with fucose of 0.5±0.3. This average molar ratio indicates that there is roughly one sulfate group for every two fucose monomers, which is in between previously reported structures of fucoidan (Patankar et al. 1993; Sichert et al. 2021). Lastly, we observe that giant kelp DOC has strong optical properties, with an absorption peak near 270nm because of its phenolic content.

Determination of DOC Microbial Remineralization Rates

Bioassay methods - Remineralization bioassays are essential to quantify the fraction of the macroalgal derived DOC that is bioavailable to microbial remineralization at surface versus how much survives degradation and potentially available for export or sequestration. Remineralization bioassay experiments are set up as seawater dilution cultures in which a source microbial assemblage (1.2 µm filtrate) are inoculated into a naturally occurring seawater media (0.2 µm filtrate) (Carlson et al. 2004). The cultures are incubated at in situ temperatures (maintained in upright incubators) in the dark for one year. We will monitor changes in DOC concentrations, total carbohydrates, sugar concentrations and total phenol content are collected

from incubations in periods from days to one year. Changes in DOC composition will determine what compounds produced by seaweed may contribute to sequestration on longer time scales.

Prototype remineralization Assays from Sargassum natans - The described remineralization assays occur on timescales greater than the time of quarterly reporting. As a proof of concept, we present data from a smaller scale remineralization bioassay (~3 months) using DOC derived from *Sargassum natans*, a brown macroalgae. DOC from *Sargassum natans* is composed of similar material to giant kelp (38% carbohydrates enriched in fucose, galactose and glucuronic acid, and 12% polyphenols). Accumulated DOC was amended to batch remineralization assays and DOC concentrations were measured over time in triplicate.

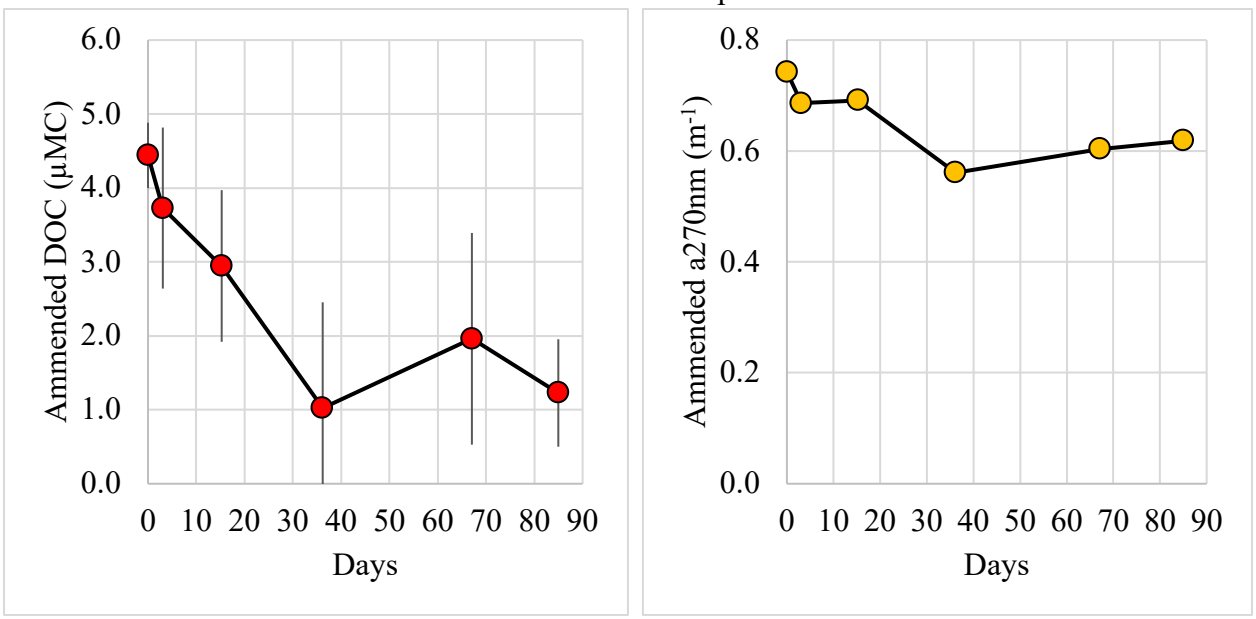

Figure 10. (a) Amended macroalgal DOC over time (b) Absorption of amended macroalgal DOC at 270nm over time. Absorption at 270nm is used as a proxy for macroalgal polyphenols

Figure 10a shows the change in amended macroalgal DOC concentrations over time. From triplicate incubations we observed that 27±10% of Sargassum DOC resists heterotrophic remineralization over the course of 3 months. We further demonstrate that polyphenols produced by macroalgae appear to contribute to the observed recalcitrance (Figure 10b). By the end of the incubation, DOC absorption at 270nm, the peak absorption of macroalgal polyphenols, was 83% of its initial value and, similar to bulk DOC, remained relatively unchanged after 30 days, indicating its possible contribution to DOC recalcitrance.

Determination of DOC Photooxidation Remineralization Rates

Methods - A handful of studies demonstrate that a fraction of seaweed derived DOC is rapidly oxidized when exposed to light (Shank et al. 2010; Wada et al. 2015). This photooxidation occurs alongside the degradation of seaweed DOC optical properties indicating polyphenols may be degraded when exposed to light (Powers 2020), limiting their potential to contribute to sequestration. Photooxidation experiments are conducted to determine the fraction of DOC that is rapidly oxidized by light in the surface ocean. Photomineralization experiments are conducted in 15-20 ml quartz vials using a LS1000W Solar Simulator (Solar Light CO. Inc). Briefly, seaweed DOC is collected and filled into quartz vials with PTFE lined caps. Experiments should be conducted at seawater salinity and pH. Samples are placed in a circulating water bath to maintain temperature and irradiated for 48 hours. Vials are sampled sacrificially at 0, 24 and 48 hours to resolve the timescale of photooxidation and are subsampled for DOC concentrations, optical properties (CDOM), total phenol content, dissolved inorganic carbon (DIC) and carbon monoxide. DOC, CDOM, TPC and DIC are measured as described above.

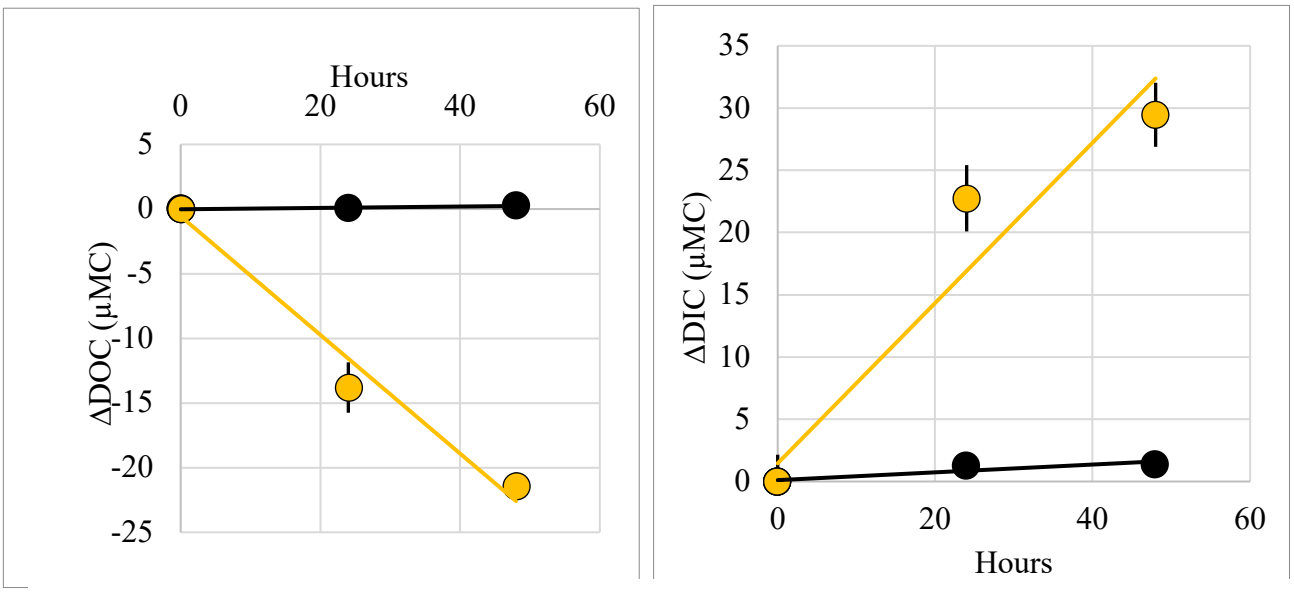

Figure 11. (a) Photooxidation of macroalgal DOC. (b) Production of CO_2, measured as total dissolved inorganic carbon, by photooxidation of macroalgal DOC. Yellow lines and circles are light exposure treatment. Black lines and circles are dark treatment.

Photooxidation Results - From incubations conducted in triplicate we observe approximately 22 ± 1.2 µM macroalgal DOC is photooxidized within 48 hours compared to the dark control treatments (Figure 11a). Correspondingly, this loss in organic carbon was balanced by the production of 29.5 ± 3.5 µMC as CO_2, measured as total dissolved inorganic carbon (Figure 11b). Out of necessity, DOC and CO_2 samples are made from separate parallel vials, and the apparent excess CO_2 production, compared to DOC loss is possibly a result of uneven light exposure in the solar simulator. Future work will be made to address how to create a more

uniform light environment. We additionally observed a decrease in the absorption of the macroalgal DOC at 270nm, indicating light oxidizes polyphenols to CO_2, limiting their potential to sequester carbon in the surface ocean.

Task 4 – Modeling the environmental impacts of seaweed cultivation and sequestration

Q4 deliverable – M4.3 – Streamlining of the MAG model – Completion level 100%

Leads: Daniel Dauhajre, Danielle Bianchi, Ahn Pham & Jim McWilliams (all UCLA) & David Siegel (UCSB)

We continue the model development targeting a virtual seaweed mCDR experiment in the Southern California Bight (M4.5-4.6). This development includes streamlining the macroalgal growth model (MAG) of Frieder et al. 2022 (M4.3); the model simplifications were partially described in the last QR and are detailed below. This streamlined MAG is presently being validated against a SBC LTER dataset and simultaneously implemented in the online coupled ROMS-BEC-MAG modeling system (Task 4.4). The short-term target remains the same as described in QR3: a publication that introduces ROMS-BEC-MAG with an idealized demonstration of upper-ocean interactions between the farm, currents, and biogeochemistry and a quantification of farm impacts and C conveyance as a function of sinking strategy.

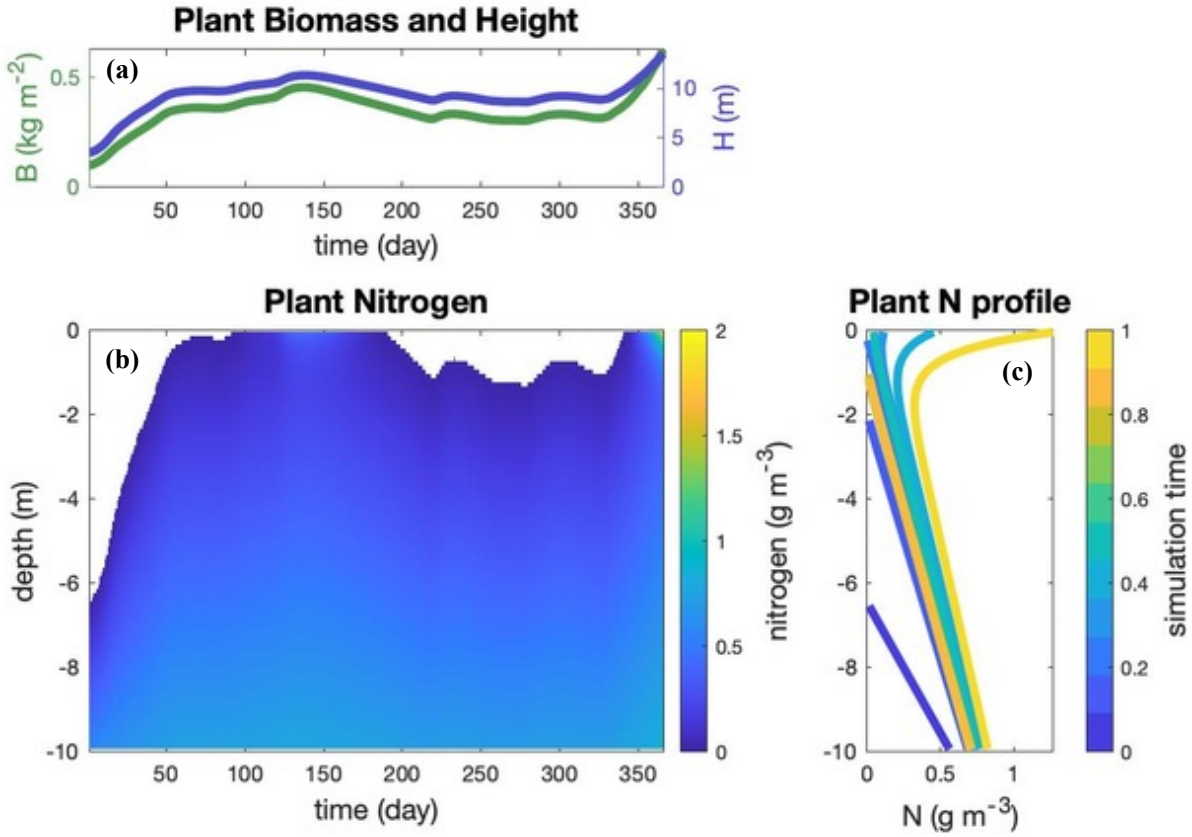

Figure 12: Demonstration of streamlined MAG model output (run in MATLAB) forced by nutrients, currents, and light in a ROMS-BEC simulation of the Southern California Bight over 1

year. (a): vertically integrated biomass (green) and simulated plant height (blue). (b): evolution in (depth,time) space of the fixed nitrogen (directly proportional to biomass). (c): evolution of the vertical biomass distribution as a function of time (colors; where 'simulation time' =1 corresponds to 365 days). Present work targets validation and tuning of rates (e.g., mortality) against SBC LTER data (see text).

The streamlined MAG model (M4.3) is presently in a MATLAB code and accessible via a (temporarily private) GitHub repository hosted by D. Bianchi. Model changes include the following: (1) an elimination of the frond tracking algorithm for (previously non-conservative with respect to N) biomass initiation or senescence; (2) parameterized frond initiation and senescence in the bulk growth and mortality terms (with rates to be tuned based on LTER validation, see below); and (3) an inverse linear power law vertical distribution function of biomass that continuously transitions from subsurface to canopy-forming profiles and approximately matches the quasi-empirically derived, non-generalized distribution functions of Frieder et al. 2022. An example of the streamlined, offline MAG output is shown in Fig. 12. A present priority is tuning the mortality term.

We are presently validating and tuning the streamlined MAG model with a SBC LTER dataset from the Arroyo Quemado kelp bed in Santa Barbara. This dataset includes a majority of the inputs for the MAG model (e.g., currents, light, nutrients) as well as a measure of depth-integrated biomass with some information on the vertical structure of the biomass (e.g., subsurface versus canopy-forming). In this manner, we will be able to validate and tune the streamlined MAG to reproduce the observed *time-series* of (vertically integrated) biomass. The temporal variability resolved in this validation exercise extends the MAG validation in Frieder et al. 2022, which only compared bulk growth rates and biomass. The streamlined MAG model, code, and its validation against SBC LTER are being written up in a white paper in anticipation of publication.

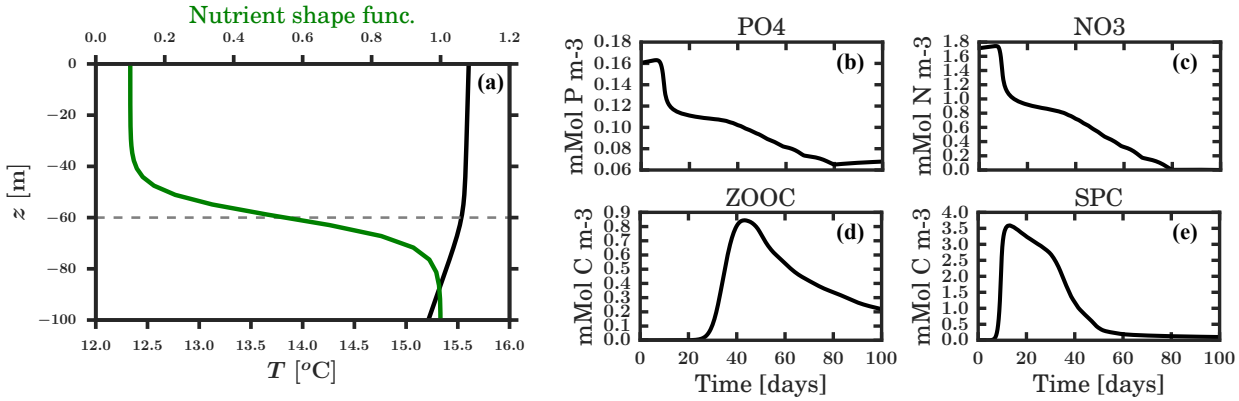

Figure 13: Test-case initial condition (a) and BEC output (b-e) for ROMS-BEC idealized channel configuration. The initial condition (a) prescribes approximately uniform temperature (black) and nutrients (green) in a surface mixed layer (dashed grey line) that transition into constant stratification and constant nutrients in the interior. The green curve in (a) shows the non-dimensional shape function used for all initial nutrient concentrations. Maxima and minima for each BEC tracer (excluding plankton) are defined relative to values in Southern California regional simulations and the shape function is maxima at the surface (and minima at the bottom) for some BEC tracers (e.g., O2). In this test-case simulation, the

physics is in a steady state, so only the biogeochemistry evolves (b-e). The time-series in b-e show evolution of the upper-ocean average of a subset of the BEC tracers: phosphorus (b), nitrate (c), zooplankton carbon (d), and small phytoplankton carbon (e).

Finally, the streamlined MAG model is being implemented in the online coupled, Fortran code (ROMS-BEC-MAG). As described in QR3, the testbed for the coupled code is an idealized channel-flow simulation. We are presently developing a ROMS-BEC baseline case for this configuration (Figure 13) to establish a baseline for net primary production and C cycling in the `natural' system. Once this baseline is established (e.g., equilibrated circulation and NPP) we will introduce a farm and vertical conveyance functionality (Task 4.4). This idealized configuration will serve as a benchmark case for public use of the ROMS-BEC-MAG code.

We have also been addressing the influence of non-instantaneous air-sea gas transfer rates on the sequestration time scales of the remineralized organic carbon for the natural biological pump (Nowicki et al. in review, GBC). This paper illustrates that assessments of sequestration of organic carbon by the biological pump is roughly 40% greater in non-instantaneous air-sea gas transfer is considered compared with instantaneous gas transfer as was used in Siegel et al. (2021). This is due to both the long equilibration time scales (months to year) of the carbonate system, the rapid subduction of surface water parcels, particularly for Subarctic Ocean regions, and biological uptake of the remineralized DIC intercepting it before it reaches the sea surface. We are working on extensions of this work that address mCDR applications including seaweed CDR. This work extends our plans on M4.6 (Assessment of sequestration time scales of the remineralized organic carbon) to more correctly the sequestration time scales of seaweed CDR.

References:

Abdullah, M. I., and S. Fredriksen. 2004. Production, respiration and exudation of dissolved organic matter by the kelp *Laminaria hyperborea* along the west coast of Norway. *J. Mar. Biol. Assoc. U. K.* **84**: 887–894. doi:10.1017/S002531540401015Xh

Box, J. D. 1983. Investigation of the Folin-Ciocalteau phenol reagent for the determination of polyphenolic substances in natural waters. *Water Res*. **17**: 511–525. doi:10.1016/0043-1354(83)90111-2

Buck-Wiese, H., M. A. Andskog, N. P. Nguyen, and others. 2023. Fucoid brown algae inject fucoidan carbon into the ocean. *Proc. Natl. Acad. Sci.* **120**: e2210561119. doi:10.1073/pnas.2210561119

Carlson, D. J., and M. L. Carlson. 1984. Reassessment of exudation by fucoid macroalgae. *Limnol. Oceanogr*. **29**: 1077–1087. doi:10.4319/lo.1984.29.5.1077

Carlson, C. A., Giovannoni, S. J., Hansell, D. A., Goldberg, S. J., Parsons, R. & Vergin, K. 2004. Interactions among dissolved organic carbon, microbial processes, and community structure in the mesopelagic zone of the northwestern Sargasso Sea. *Limnology and Oceanography,* 49**,** 1073-1083

Engel, A., and N. Händel. 2011. A novel protocol for determining the concentration and composition of sugars in particulate and in high molecular weight dissolved organic matter (HMW-DOM) in seawater. *Mar. Chem*. **127**: 180–191. doi:10.1016/j.marchem.2011.09.004

Frieder, C.A., Yan, C., Chamecki, M., Dauhajre, D., McWilliams, J.C., Infante, J., McPherson, M.L., Kudela, R.M., Kessouri, F., Sutula, M. and Arzeno-Soltero, I.B., 2022. A Macroalgal cultivation modeling system (MACMODS): evaluating the role of physical-biological coupling on nutrients and farm yield. *Frontiers in Marine Science*, *9*, p.752951. https://doi.org/10.3389/fmars.2022.752951.

Jennings, J. G., and P. D. Steinberg. 1994. In situ exudation of phlorotannins by the sublittoral kelp Ecklonia radiata. *Mar. Biol*. **121**: 349–354. doi:10.1007/BF00346744

Krause, S.J.E., Dauhajre, D.P., Bell, T., Miller, R., Valentine, D. and Siegel, D., 2023. Comparing kelp conveyance strategies for marine carbon dioxide removal with farmed macroalgae. White paper available at https://doi.org/10.31223/X5M66B.

Nelson, C. E. 2013. Coral and macroalgal exudates vary in neutral sugar composition and differentially enrich reef bacterioplankton lineages. *ISME J*. 18.

Nowicki, M., T. DeVries, and D.A. Siegel, in review, The influence of air-sea CO_2 disequilibrium on carbon sequestration by the ocean's biological pump.

Patankar, M. S., S. Oehninger, T. Barnett, R. L. Williams, and G. F. Clark. 1993. A revised structure for fucoidan may explain some of its biological activities. *J. Biol. Chem*. **268**: 21770–21776. doi:10.1016/S0021-9258(20)80609-7

Powers, L. C., N. Hertkorn, N. McDonald, P. Schmitt-Kopplin, R. D. Vecchio, N. V. Blough, and M. Gonsior. 2019. Sargassum sp. Act as a Large Regional Source of Marine Dissolved Organic Carbon and Polyphenols. *Glob. Biogeochem. Cycles* **33**: 1423–1439. doi:10.1029/2019GB006225

Reed, D. C., C. A. Carlson, E. R. Halewood, J. C. Nelson, S. L. Harrer, A. Rassweiler, and R. J. Miller. 2015. Patterns and controls of reef-scale production of dissolved organic carbon by giant kelp Macrocystis pyrifera. *Limnol. Oceanogr.* **60**: 1996–2008. doi:10.1002/lno.10154

Shank, G. C., R. Lee, A. Vähätalo, R. G. Zepp, and E. Bartels. 2010. Production of chromophoric dissolved organic matter from mangrove leaf litter and floating Sargassum colonies. Mar. Chem. **119**: 172–181. doi:10.1016/j.marchem.2010.02.002

Sichert, A., S. Le Gall, L. J. Klau, B. Laillet, H. Rogniaux, F. L. Aachmann, and J.-H. Hehemann. 2021. Ion-exchange purification and structural characterization of five sulfated fucoidans from brown algae. *Glycobiology* **31**: 352–357. doi:10.1093/glycob/cwaa064

Siegel, D.A., T. DeVries, S.C. Doney and T. Bell, 2021, Assessing the sequestration time scales of some ocean-based carbon dioxide reduction strategies. *Environmental Research Letters*, https://doi.org/10.1088/1748-9326/ac0be0.

Takeda, K., M. Moriki, W. Oshiro, and H. Sakugawa. 2013. Determination of phenolic concentrations in dissolved organic matter pre-concentrate using solid phase extraction from natural water. *Mar. Chem.* **157**: 208–215. doi:10.1016/j.marchem.2013.10.008

Wada, S., M. N. Aoki, Y. Tsuchiya, T. Sato, H. Shinagawa, and T. Hama. 2007. Quantitative and qualitative analyses of dissolved organic matter released from Ecklonia cava Kjellman, in Oura Bay, Shimoda, Izu Peninsula, Japan. *J. Exp. Mar. Biol. Ecol*. **349**: 344–358. doi:10.1016/j.jembe.2007.05.024

Zhao, Z.-F., Z.-J. Huang, Z.-D. Sun, and others. 2023. Effects of instantaneous changes in temperature, light, and salinity on the dynamics of dissolved organic carbon release by Sargassum thunbergii. *Mar. Pollut. Bull*. **190**: 114865. doi:10.1016/j.marpolbul.2023.114865

SeaweedCDR Publications to Date:

Peer Reviewed Journal Articles:

Nowicki, M., T. DeVries, and D.A. Siegel, in review, The influence of air-sea CO_2 disequilibrium on carbon sequestration by the ocean's biological pump.

Project White Papers with DOI's:

Dauhajre, D.P., Bell, T. and Siegel, D., 2023. Considerations for Regional Simulations of Seaweed Carbon Dioxide Removal. White paper available at https://doi.org/10.31223/X52Q1N.

Krause, S.J.E., Dauhajre, D.P., Bell, T., Miller, R., Valentine, D. and Siegel, D., 2023. Comparing kelp conveyance strategies for marine carbon dioxide removal with farmed macroalgae. White paper available at https://doi.org/10.31223/X5M66B.

English, C.J. and Carlson, C.A., 2023. Protocols for the quantification and characterization of dissolved organic carbon from seaweed and its sequestration potential. White paper available at https://doi.org/10.31223/X5167F.